Applications of Symbolic Dynamics to Differential Chaos Shift Keying

Gian Mario Maggio, *Member IEEE,*
Zbigniew Galias, *Member IEEE*

Abstract

In this paper we propose an enhanced version of the DCSK (Differential Chaos Shift Keying) scheme where the carrier symbolic dynamics are exploited for conveying useful information. This is achieved by means of a pseudo-chaotic encoder which spreads the input sequence approximating the dynamics of the Bernoulli shift. The information encoded in the pseudo-chaotic carrier is retrieved by using standard maximum-likelihood detection. It is shown that the proposed method can also be useful for noise filtering purposes.

Keywords

DCSK (Differential Chaos Shift Keying), Symbolic dynamics, Noise filtering, Trans-information.

I. Introduction

Among the several proposed chaos-based communication schemes DCSK (Differential Chaos Shift Keying) [1], [2], [3], exhibits one of the best BER performances and it has been shown to be particularly robust against multipath fading [4]. In DCSK, for each symbol period, a portion of chaotic waveform (reference signal) is transmitted followed by its inverted or non-inverted copy (information-bearing signal) depending on the bit of information. At the receiver, the information is extracted by means of differentially coherent demodulation, that is by correlating the information-bearing part of the signal with the reference. However, as pointed out in [5], [6], part of the information associated with the chaotic carrier remains unexploited. We emphasize that a chaotic system may be seen as an information source, which reveals more and more information about its initial state during the evolution in time [7]. Actually, the entropy associated with a chaotic signal can be measured by introducing the formalism of symbolic dynamics [8]. For piecewise linear Markov (PWLM) maps there exists a natural discretization which allows to define a one-to-one relationship between any initial condition and an (infinite) symbolic sequence [9].

In DCSK the total channel capacity is shared between the payload bits transmitted and the symbolic sequence, which is also transmitted (in a hidden way), associated with the chaotic carrier. Furthermore, the two sources are clearly independent [6]. In this work we propose an enhanced version of DCSK, which we call SD-DCSK, exploiting the symbolic dynamics (SD) associated with the chaotic carrier. This is obtained by replacing the chaotic generator used in DCSK with a pseudo-chaotic (PC) encoder [10], [11], which generates a chaotic signal from the original input sequence. In practice, the pseudo-chaotic encoder is realized with a convolutional-like encoder followed by a DAC (digital/analog converter), approximating the iterates of the chaotic Bernoulli shift [12]. We show that the information encoded in the pseudo-chaotic carrier can be extracted efficiently using standard maximum-likelihood detection. Also, the corresponding trellis exhibits an interesting scalability property deriving directly from the symbolic dynamics approach.

The SD-DCSK scheme allows the creation of an auxiliary communication channel, in parallel to the DCSK one. This can be used to increase the data rate of the system by transmitting independent information. If instead the same binary stream is sent as for DCSK, it can be employed for error-correction purposes [13]. In addition, the recovered information associated with the symbolic dynamics of the (pseudo-)chaotic carrier may be used to "clean" the reference part of the DCSK signal, thus improving the BER (bit error rate)

G.M. Maggio is with the Center for Wireless Communications (CWC), UC San Diego, La Jolla, CA 92093-0407, USA, e-mail: gmaggio@ucsd.edu. Corporate affiliation with STMicroelectronics, Inc., AST-La Jolla, e-mail: gian-mario.maggio@st.com.

Z. Galias is with the Department of Electrical Engineering, University of Mining and Metallurgy, al. Mickiewicza 30, 30–059 Kraków, Poland, e-mail: galias@zet.agh.edu.pl.

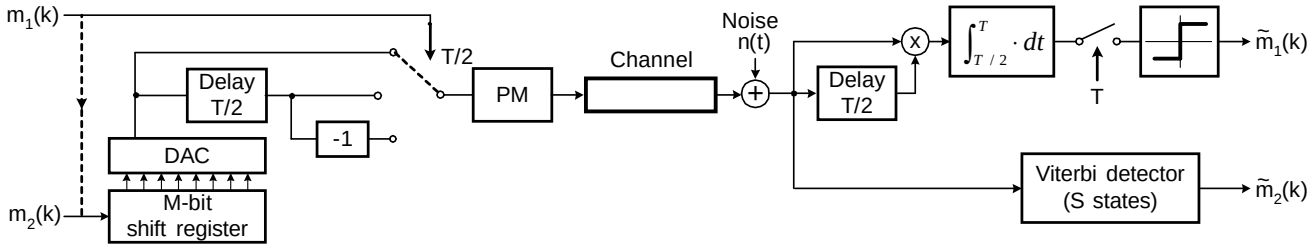

Fig. 1. Simplified block diagram of the SD-DCSK scheme. For forward error-correction applications: $m_2(k) \equiv m_1(k)$.

performance of DCSK as a communication system. Finally, we characterize the improvement in terms of the total transfer of information between transmitter–receiver in terms of trans-information [15].

The paper is structured as follows. In Sec. II we present the relevant theory concerning the encoding/decoding of the information exploiting symbolic dynamics. Sec. III reports the simulation results for the SD-DCSK scheme in terms of BER performance. In Sec. IV we demonstrate the noise-filtering capabilities intrinsic in the SD-DCSK system. Finally, the results regarding the computation of the trans-information are reported in Sec. V.

II. SD-DCSK

The basic idea behind the SD-DCSK scheme is to replace the chaos generator present in the DCSK scheme [2] with a pseudo-chaotic encoder, as illustrated schematically in Fig. 1. We denoted with $m_1(k)$ the binary stream to be modulated according to the original DCSK scheme. On the other hand, the input sequence $m_2(k)$ is used to generate the pseudo-chaotic carrier. Note that the inputs m_j $(j = 1, 2)$ are independent from each other, although the same sequence can be transmitted in both channels in order to increase the reliability of the communication. The only assumption that is made is on $m_2(k)$ to be an i.i.d. (independent identically distributed) sequence, as discussed later.

A. Pseudo-Chaotic Encoder

The PC-encoder performs a spreading of the input sequence $m_2(k)$, mimicking the chaotic dynamics of the Bernoulli shift map, defined by [12]:

$$x_{k+1} = 2x_k \mod 1 \tag{1}$$

whose graph is shown in Fig. 2. The state x can be represented as a binary expansion:

$$x = 0.b_1b_2b_3\ldots \equiv \sum_{j=1}^{\infty} 2^{-j}b_j \tag{2}$$

where each of the bits b_j is either a "0" or a "1", and $x \in I = [0, 1]$. The successive iterates of x are obtained by moving the separating point one position to the right (multiplication by 2) and setting to zero the integer digit (modulo 1 operation). Hence, digits which are initially far to the right of the separating point, thus having only a very slight influence on the value of x, eventually become the first fractional digit. The information is encoded by associating the symbol "0" to the subinterval $I_0 = [0, 0.5)$ and the symbol "1" to $I_1 = [0.5, 1]$, as shown in Fig. 2.

In this work the Bernoulli shift process is approximated by means of an M-bit shift register followed by a DAC, as illustrated in Fig. 1. Correspondingly, the generic state x_l (with $l = 1, 2, \ldots, 2^M$) can be expressed as:

$$x_l = 0.b_1b_2\ldots b_M \equiv \sum_{j=1}^{M} 2^{-j}b_j \tag{3}$$

where b_1 and b_M represent the MSB (most significant bit) and the LSB (least significant bit), respectively. The shift operation corresponds to a multiplication by a factor 2, while the modulo 1 operation is realized by

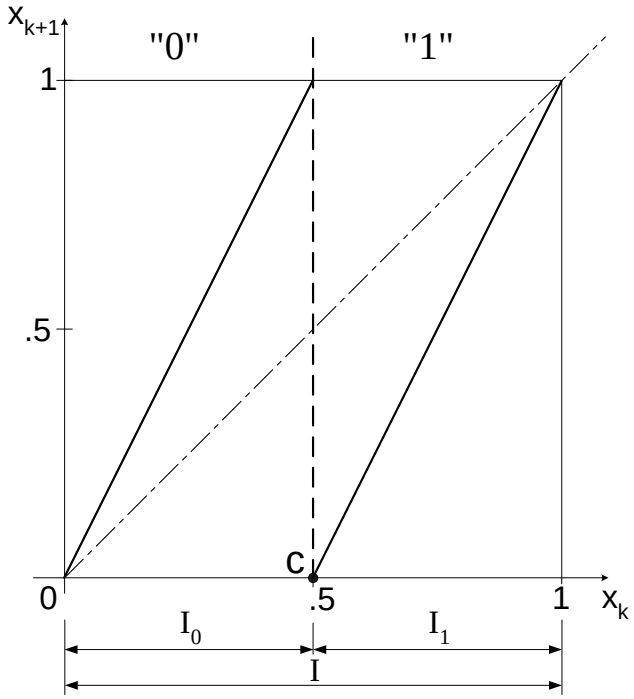

Fig. 2. The Bernoulli shift map with its definition of symbolic dynamics. The invariant interval $I = [0, 1]$ is partitioned with respect to the critical point $c = 0.5$. The subintervals I_0 and I_1 are assigned the binary symbols "0" and "1", respectively.

discarding the shifted MSB at each step. The shift register is fed with the input sequence $m_2(k)$, which we assume to be i.i.d.[1] At each step the most recent bit of information is assigned the LSB position while the old MSB is discarded. Due to the finite length of the shift register, the dynamics of the Bernoulli shift can only be approximated. In particular, for an M-bit shift register the quantization error ε is bounded from above by $\varepsilon(M) < 2^{-M}$, which tends to zero for $M \to \infty$.

From the viewpoint of information theory the shift register structure implementing the Bernoulli shift may be seen as a form of convolutional coding [14]. The memory of the structure is represented by the shift register which stores the last M input bits. Each input bit causes an output of M bits; thus, the overall code rate is $1/M$.

In general, the shift register implementing the Bernoulli shift map may be followed by a transformation unit for generating more complex chaotic maps. For example, a Gray/Binary converter can be used to generate the tent map.

B. SD-DCSK Modulation

In order to describe the SD-DCSK modulation we consider a discrete-time baseband model of a DCSK telecommunication system. This model can be shown to be equivalent to sampling the continuous-time DCSK signal transmitted over an RF (radio frequency) bandlimited channel, employing phase modulation (PM). In particular, in this work we consider DCSK for the case $L = 1$, which means that for each symbol period T one (pseudo-)chaotic iterate is generated [2]. Hence the data rates associated with $m_1(k)$ and $m_2(k)$ in this case coincide. However, note that in general the transmission rate associated with the SD channel ($m_2(k)$) would be L-times larger than the DCSK channel ($m_1(k)$).

By denoting with x_k the k-th pseudo-chaotic iterate, we define the corresponding symbol s_k as follows:

$$s_k = [\cos(\varphi_k), \sin(\varphi_k)] \tag{4}$$

where: $\varphi_k = 2\pi x_k + \varphi_0$, and $\varphi_0 = 2\pi/2^{M+1}$, is a phase offset chosen accordingly with the definition of

[1]In practice this may be achieved by inserting a data compression and/or a data scrambling block in front of the shift register.

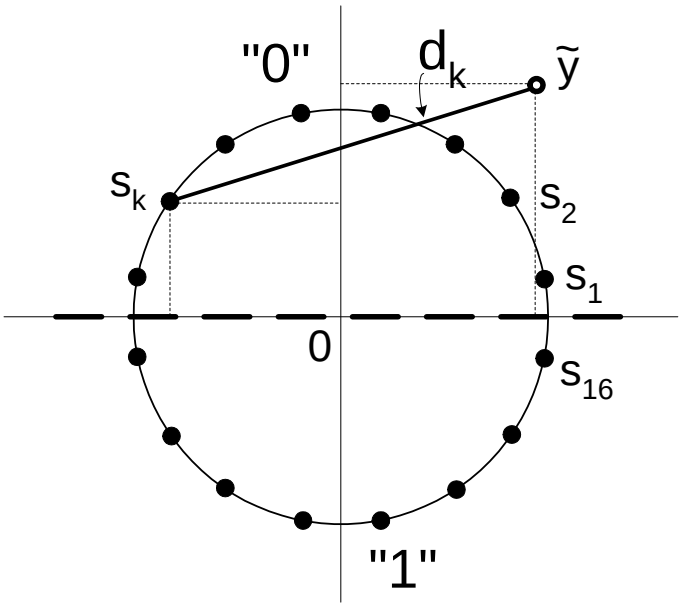

Fig. 3. Signal-space diagram for the SD-DCSK transmitted signal ($M = 4$ bits) illustrating the geometrical meaning of the branch metric d_k. Note also that the arc $[0, \pi)$ is associated with the symbol "0", while $[\pi, 2\pi)$ corresponds to the symbol "1".

the decision boundaries. Note that the symbol definition (4) guarantees that the transmitted energy/bit is constant. The corresponding signal-space diagram is shown in Fig. 3. Also, with these notations $\varphi_k \in [0, 2\pi]$; thus the invariant interval $I = [0, 1]$ of the Bernoulli shift, with its definition of symbolic dynamics, maps to the unit circle in the signal space.

Then, by denoting with E_b the energy/bit, in the first half $[0, T/2]$ of the symbol period we transmit the reference vector:

$$Y = [Y_1, Y_2] = \left[\sqrt{\frac{E_b}{2}} \cos(\varphi_k), \sqrt{\frac{E_b}{2}} \sin(\varphi_k) \right]$$

followed by $\pm Y$ in the second half $[T/2, T]$, depending on the input bit $m_1(k)$. An example of transmitted SD-DCSK signal and its spectrum are illustrated in Fig. 4, in normalized units. We emphasize that for practical applications (and assuming $m_2(k)$ to be an i.i.d. sequence) the pseudo-chaotic signal can be considered equivalent to the one produced by a real chaos generator.

C. SD-DCSK Demodulation

The scheme proposed allows the creation of an auxiliary communication channel to the DCSK one, exploiting the symbolic dynamics associated with the chaotic carrier. As far as the demodulation is concerned, the two channels can be considered independent from each other.

C.1 DCSK

Referring to Fig. 1, the DCSK demodulation is carried out as usual, *i.e.* by correlating the information-bearing part of the signal ($t \in [T/2, T]$) with the reference ($t \in [0, T/2]$), sampling the correlator output according to the symbol period T, and inferring on the symbol received by means of a threshold detector [2].

C.2 SD Decoder

The information encoded in the pseudo-chaotic carrier can be extracted from the received signal by considering its reference part only. In the simplest case the pseudo-chaotically encoded data can be detected by a phase discriminator detecting whether $\varphi_k \in [0, \pi]$ or $[\pi, 2\pi]$, respectively (see Fig. 3). This method is not very effective as it relies solely on the sign of the sample Y_2. In addition, because of the signal-space diagram

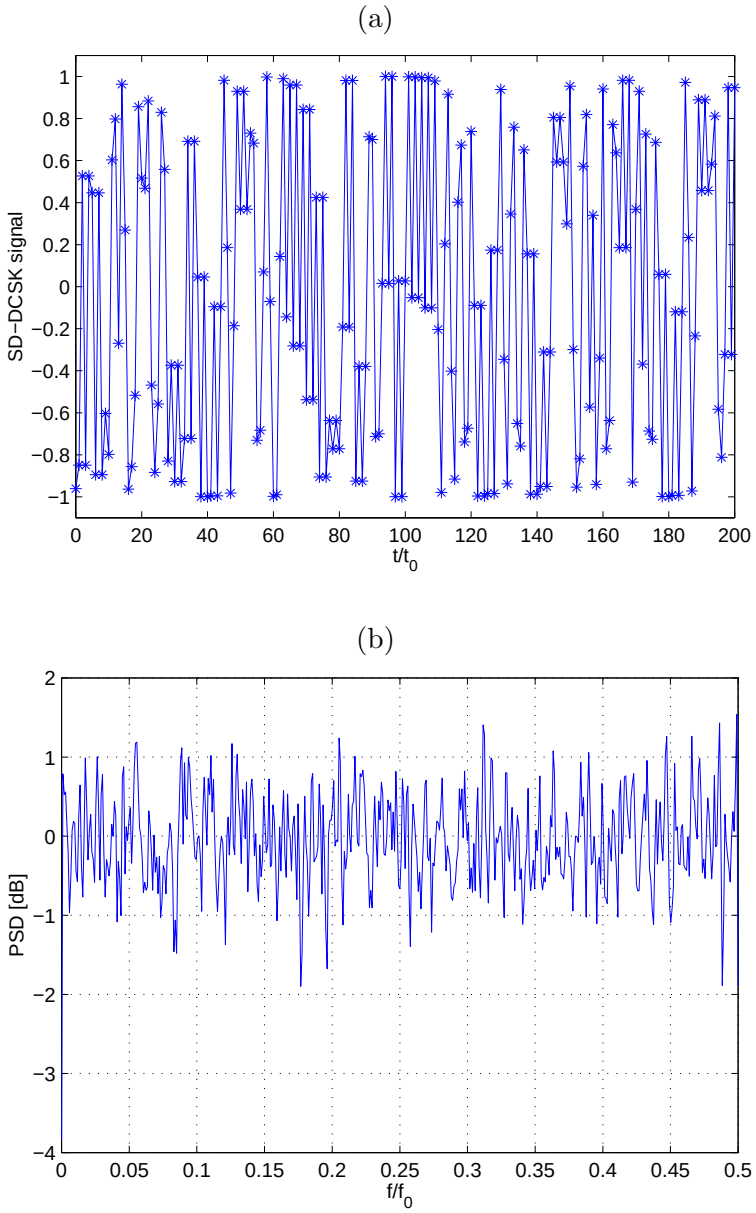

Fig. 4. (a) Transmitted SD-DCSK signal ($M = 10$ bits), and (b) corresponding PSD (power spectral density). The plots refer to normalized time t/t_0 and normalized frequency f/f_0, where $t_0 = 1/f_0$ is the sampling period.

associated with the PC-encoder, symbols such that $\sin(\varphi_k) \approx 0$ will cause an error also for relatively low noise levels.

On the other hand, the SD signal is amenable of maximum-likelihood detection. By assuming the input $m_2(k)$ to be an i.i.d. sequence, the optimal decoder for the PC-encoded signal is represented by a trellis matched to the dynamics of the Bernoulli shift, seen as convolutional encoder. In fact, we recall that every PWLM map admits a representation as a topological Markov chain [9]. In this work we consider soft Viterbi decoding and for illustrating the branch metric computations we consider the normalized vector: $y = \sqrt{2/E_b}Y$. At each step, the input of the Viterbi algorithm is a vector $\tilde{y} = [\tilde{y_1}, \tilde{y_2}]$ representing the received symbol affected by noise. By assuming that each sample is perturbed by an independent Gaussian variable (AWGN) it can be shown that the observation probability of receiving $\tilde{y}$, if the symbol $s_k = [s_{k1}, s_{k2}]$ was sent, is proportional to $e^{\left((\tilde{y_1}-s_{k1})^2+(\tilde{y_2}-s_{k2})^2\right)/2\sigma_n^2}$ where σ_n is the noise variance. This in terms of logarithms, according to the usual

formulation of the Viterbi algorithm, translates into the following branch metric:

$$d_k = \sqrt{(\tilde{y_1} - s_{k1})^2 + (\tilde{y_2} - s_{k2})^2} \tag{5}$$

whose geometrical interpretation is shown in Fig. 3.

Note that the same PC-encoded signal can be decoded by Viterbi detectors with different number of states. This is a direct consequence of the symbolic dynamic approach used for encoding/decoding information in the pseudo-chaotic carrier. Namely, given the number $N(= 2^M)$ of transmitter levels, the received PC-signal can be decoded with Viterbi detectors with $S = 2, 4, 8 \ldots, N$ states. This requires a slight modification in the branch metric computation; in particular, in this work we compute the observation probabilities based on the transmitter level "closest" to the received signal. We reiterate that the scalability property allows to perform a high spreading at the transmitter (large N) such that the PC-iterates reproduce with very good approximation the dynamics of the Bernoulli shift, while decoding with reduced complexity (small S). Of course, the performance of the Viterbi detector depends on the number of states, as discussed in the next section.

III. BER Performance

The results of our analysis are presented in terms of BER probability versus the ratio E_b/N_0 expressed in dB, where E_b is the energy per user bit—which coincides for $m_1(k)$ and $m_2(k)$—and N_0 is the single-sided spectral noise density. We consider here the interference on the channel to be just AWGN (additive white Gaussian noise).

Fig. 5 shows the simulation results for the auxiliary communication channel associated with the pseudo-chaotic carrier, versus DCSK. The BPSK (binary phase shift keying) curve is also shown for reference purposes. We observe that soft Viterbi decoding results in a good BER performance, that is significantly better than DCSK, even though the energy associated with the information bearing part of the signal is not utilized. Of course, to make a fair comparison one should take into account that DCSK it is an uncoded modulation, while SD channel benefits from the coding gain resulting from the pseudo-chaotic encoder. Still, these results indicate that in conventional DCSK a considerable amount of information transmitted over the channel is not exploited for communication purposes.

Note the BER dependence on the number S of states in the Viterbi detector, confirming the scalability property discussed above. Also, we note a saturation effect in the performance when increasing the number of states above a certain number (in the example $S = 32$).

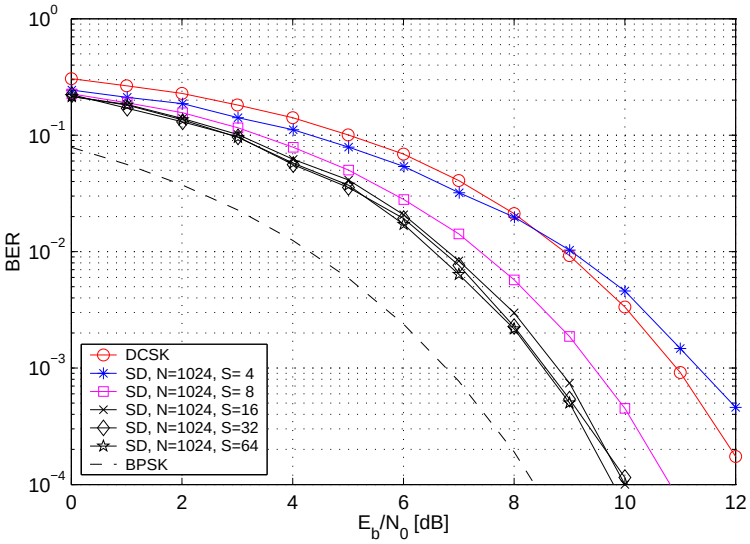

Fig. 5. BER performance: DCSK versus pseudo-chaotic modulation. Note the dependence on the number of states S in the Viterbi detector. The BPSK curve is also shown for reference purposes.

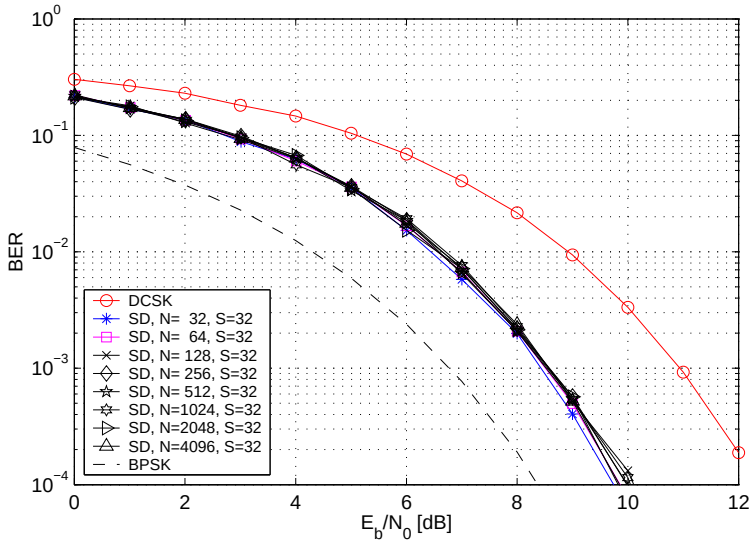

Fig. 6. BER dependence on the number N of transmitter levels, for a fixed complexity ($S = 32$) of the Viterbi detector. Note that the performance is basically independent from the number of transmitter levels.

On the other hand, Fig. 6 illustrates the BER dependence on the number N of transmitter levels, for a given receiver complexity, *i.e.* a given number of states of the Viterbi detector. Note that the performance is basically related only to the number S of states. This allows to define arbitrarily many transmitter levels, in order to minimize the quantization error, without compromising the overall performance of the auxiliary SD channel.

IV. Applications to Noise Cleaning

In the literature several methods have been proposed for the filtering of chaotic signals affected by noise [16], [17], [18], [19], [20], [21]. In this work we demonstrate how the decoded information from the SD channel can be usefully employed to "clean" the reference part of the DCSK signal, thus improving the corresponding BER performance. To this purpose the block diagram of Fig. 1 should comprise at the output $\tilde{m}_2(k)$ a serial/parallel converter followed by a DAC, whose output can be used to replace the reference part of the DCSK signal prior to the differentially coherent demodulation.[2] Fig. 7(a) shows the BER performance improvement obtained by applying the simple cleaning algorithm described above. The improvement amounts to approximately 1dB when the BER is 10^{-3}. This to the best of our knowledge is better than previously proposed methods.

The filtering technique proposed can also be applied in the context of conventional DCSK communication system, provided that maximum-likelihood detection can be performed on the chaotic carrier. To demonstrate this we consider a DCSK system using the Bernoulli shift as chaos generator, thus producing real-valued (vs. discretized) chaotic iterates. In this situation the same apparatus described for the SD-DCSK scheme can be used to produce a cleaner version of the reference signal. The corresponding results in terms of BER performance are shown in Fig. 7(b). Again, the improvement obtained is about 1dB when the error probability is 10^{-3}. This result also indicates that the fact that the transmitted iterates are not quantized practically does not affect the performance of the cleaning algorithm.

V. Computation of the Channel Trans-Information

We now consider how much information can be conveyed through the SD-DCSK channel, comparing it to conventional DCSK. To this purpose, rather than relying on the BER, we consider as a measure of the information transfer the so-called *trans-information* (or *mutual information*). In mathematical terms, the trans-information I expresses the information that two linked random variable X and Y give about each

[2]It should be clear that in general it is not possible to clean the information bearing part of the DCSK signal, because of this would require the knowledge of the transmitted information itself.

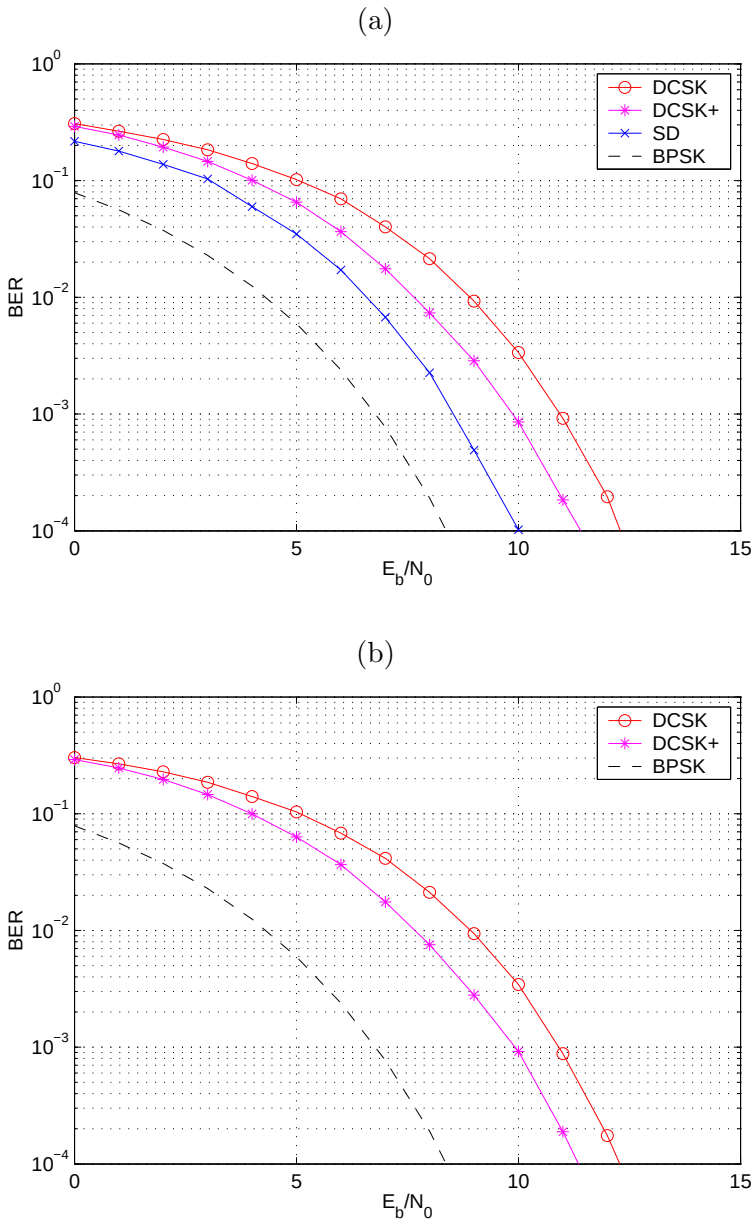

Fig. 7. Noise cleaning utilizing symbolic dynamics. (a) BER curves for SD-DCSK with and without cleaning the reference signal ($N = 1024$, $S = 32$); (b) BER curves for DCSK with and without noise filtering ($N = 1024$, $S = 32$), when a true Bernoulli shift map is used at the transmitter. Note that in both cases the improvement amounts to approximately 1dB when the error probability is 10^{-3}. The BPSK curve is also shown for comparison purposes.

other, that is [15]:

$$I(X;Y) = H(X) - H(X|Y) \tag{6}$$

with H being the entropy.

The results of our analysis for the SD-DCSK communication system, when the transmitted energy/bit is constant are summarized in Fig. 8. Namely, Fig. 8(a) shows a comparison of the BER performance for the SD versus the DCSK channel. More interestingly, in Fig. 8(b) it is shown a plot of the trans-information for the SD and DCSK channel, separately, plus the total (SD+DCSK) information transfer. From Fig. 8(b) we observe that both SD and DCSK curves saturate to 0.25 bits corresponding to the fact that for each channel ($m_1(k)$ and $m_2(k)$) four samples are transmitted for each bit. Consequently, the total trans-information curve saturates at 0.5 bits, for arbitrary large values of the signal/noise ratio.

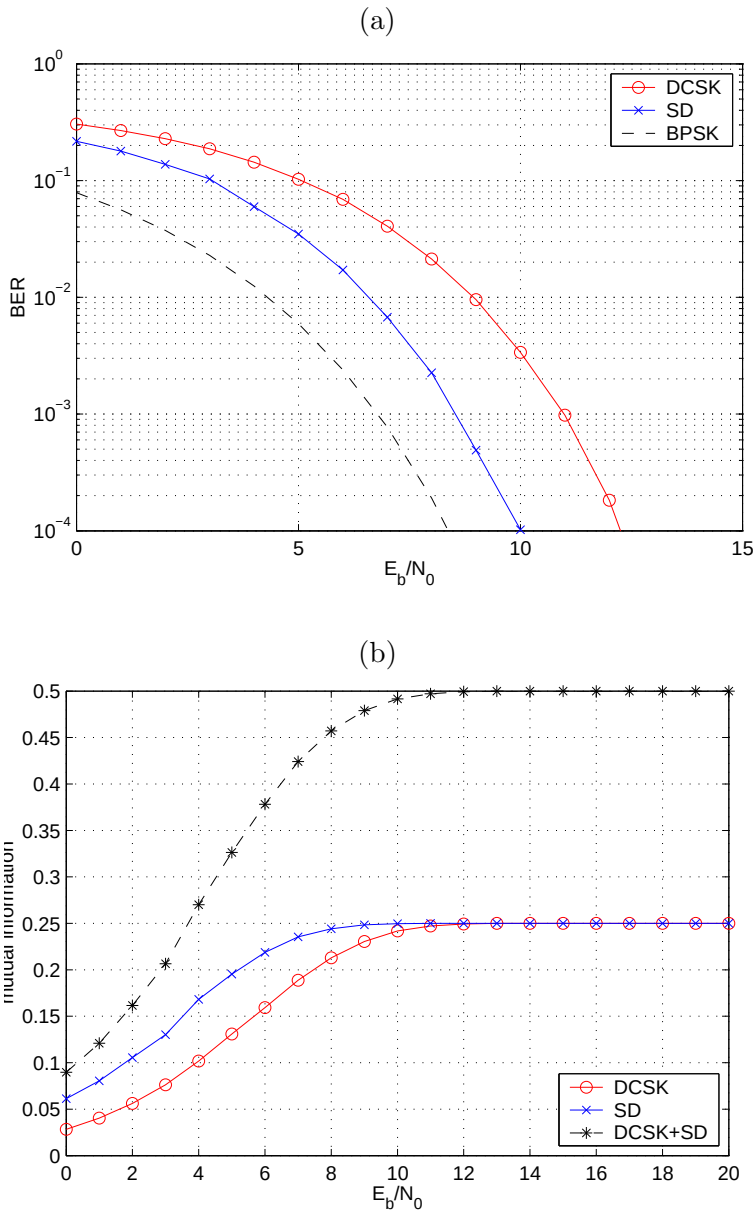

Fig. 8. SD versus DCSK when the transmitted energy per bit is constant: (a) Comparison of the BER performances, and (b) Plot of the trans-information as a function of E_b/N_0 for the SD channel, DCSK channel, and the total (SD+DCSK) information conveyed by the physical channel.

Finally, for the sake of curiosity, we show in Fig. 8 the corresponding analysis when the energy/bit is *not* constant, that is when we use AM (amplitude modulation) rather than PM (phase modulation). As expected in these conditions, while the performance of the DCSK channel is significantly degraded, the SD channel is basically maintained unaltered. This is due to the fact that the metric computations in the Viterbi detector are not affected by the nature of the signal. In other words, for the SD channel $E_b \neq const.$ basically does not change the relative distance between symbols, thus its performance. This is confirmed by Fig. 8(a), while in Fig. 8(b) this reflects into the DCSK trans-information curve saturating much slower than the SD one, when the signal/noise ratio grows indefinitely. Note also that in this case, as two samples are transmitted for each bit, the single trans-information curves tend to 0.5 bits, while the total to 1 bit.

VI. Conclusions

In this work we have proposed an enhanced version of the DCSK scheme which takes advantage of the symbolic sequence associated with the chaotic carrier for conveying useful information. This allows the

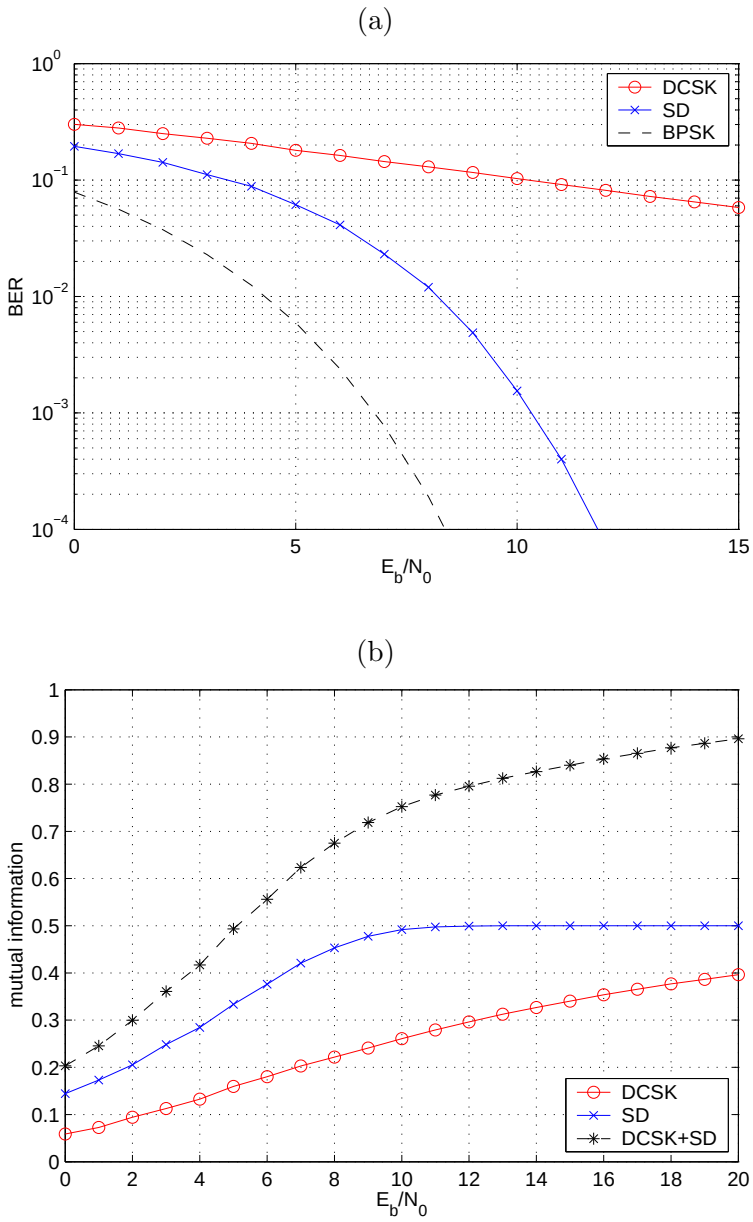

Fig. 9. SD versus DCSK when the transmitted energy per bit is *not* constant: (a) Comparison of the BER performances, and (b) Plot of the trans-information as a function of E_b/N_0 for the SD channel, DCSK channel, and the total (SD+DCSK) information conveyed by the physical channel. Note the good performance exhibited by the SD communication channel even when the energy/bit is not constant.

creation of an auxiliary communication channel to the DCSK one which can be used to increase the overall data rate and/or for error-correction purposes. As a byproduct of this analysis we have also shown how the carrier symbolic dynamics can be used to perform noise cleaning, thus improving the performance of the DCSK channel.

Acknowledgments

This work is sponsored in part by ARO (Army Research Office), grant No. DAAG55-98-1-0269.

References

[1] G. Kolumbán, M.P. Kennedy, and L.O. Chua. The role of synchronization in digital communication using chaos—Part I: Fundamentals of Digital Communications. *IEEE Trans. Circ. Syst. I*, 44(10):927–936, 1997.

[2] G. Kolumbán, M.P. Kennedy, and L.O. Chua. The role of synchronization in digital communication using chaos—Part II: Chaotic modulation and chaotic synchronization. *IEEE Trans. Circ. Syst. I*, 45(11):1129–1140, 1998.

[3] G. Kolumbán, G. Kis, Z. Jákó and M.P. Kennnedy. FM-DCSK: A robust modulation scheme for chaotic communications. *IEICE Trans. Fundamentals of Electronics, Communications and Computer Sciences*, vol. E-81A, pp. 1798–1802, 1998.

[4] G. Kolumbán and G. Kis. Multipath performance of FM-DCSK chaotic communications system. In *Proc. ISCAS 2000*, pp. 433–436, Geneva, Switzerland, May 2000.

[5] A. Abel and W. Schwarz, Maximum likelihood detection of symbolic dynamics in communication systems with Chaos Shift Keying. In *Proc. NDES 2000*, Catania, Italy, May 18-20 2000.

[6] T. Schimming, Chaos based modulations from an information theory perspective. In *Proc. ISCAS 2001*, Sydney, Australia, May 6-9 2001.

[7] R. Shaw, "Strange attractors, chaotic behavior and information flow," *Z. Naturforschung A*, vol. 36A, no. 1, 1981.

[8] B. Hao and W. Zheng, *Applied Symbolic Dynamics and Chaos*, World Scientific, Singapore, 1998.

[9] A. Lasota, M.C. MacKey, J.E. Marsden and L. Sirovich, *Chaos, Fractals, and Noise: Stochastic Aspects of Dynamics*, Springer Verlag, New York, 1994.

[10] G.M. Maggio and L. Reggiani, Applications of symbolic dynamics to UWB implulse radio. In *Proc. ISCAS 2001*, Sydney, Australia, May 6-9 2001.

[11] G.M. Maggio, N. Rulkov and L. Reggiani, Pseudo-chaotic time hopping for UWB impulse radio. *To appear in the IEEE Trans. Circ. Syst. I* (Dec 2001).

[12] E. Ott, *Chaos in Dynamical Systems*, Cambridge University Press, Cambridge (U.K.), 1993.

[13] J.G. Proakis. *Digital communications*. 3rd ed., McGraw-Hill, New York, 1995.

[14] D. Lind and B. Marcus, *An introduction to symbolic dynamics and coding*, Cambridge University Press, 1995.

[15] D.J.C. MacKay, *Information Theory, Pattern Recognition and Neural Networks*, To appear in print 2001, `http://wol.ra.phy.cam.ac.uk/mackay/itprnn/`.

[16] J. Schweizer, "Non-linear filtering for communication with chaos," *In Proc. MTNS'98*, Padova, Italy, July 1998.

[17] H. Dedieu and J. Schweizer. Noise reduction in chaotic time series–An overview. *In Proc. NDES'98*, Budapest, Hungary, June 1998.

[18] T. Schimming and M. Hasler. Constrained and unconstrained noise reduction on chaotic trajectories. *In Proc. NDES'99*, Denmark, July 1999.

[19] T Schimming, H. Dedieu, M. Hasler and M. Ogorzalek, Noise Filtering in chaos-based communication, In *Chaotic Electronics in Telecommunications*, Ed. M. P. Kennedy, R. Rovatti, G. Setti, CRC Press, 2000.

[20] Z. Jákó, G. Kolumbán and H. Dedieu, "On some recent developments of noise cleaning algorithms for chaotic signals," IEEE Trans. Circuits and Systems–Part I, vol. 47, no. 9, pp. 1403-1407, September 2000.

[21] Z. Jákó and G. Kis, "Application of noise reduction to chaotic communications: A case study," IEEE Trans. Circuits and Systems–Part I, vol. 47, no. 12, pp. 1720-1725, December 2000.